



CNS Report

ISSN 1343-2230

CNS-REP-27
KEK-Rep 2000-88
December, 2000

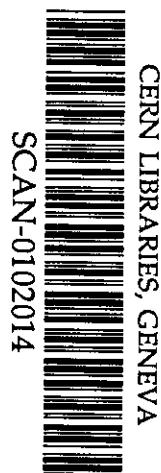
Observation of ρ/ω Meson Modification in Nuclear Matter

K. Ozawa for E325 collaboration

*Center for Nuclear Study, Graduate School of Science, the University of Tokyo
7-3-1, Hongo, Bunkyo-Ku, Tokyo 113-0033, Japan*

Center for Nuclear Study(CNS)

Graduate School of Science, the University of Tokyo
7-3-1 Hongo, Bunkyo-ku, Tokyo, 113-0033, Japan
Correspondence: cnsoffice@cns.s.u-tokyo.ac.jp



2241294

OBSERVATION OF ρ/ω MESON MODIFICATION IN NUCLEAR MATTER

K. Ozawa* , H. En'yo, H. Funahashi, M. Kitaguchi, M. Ishino[†] , H. Kanda[‡] , S. Mihara[†],
T. Miyashita[§] , T. Murakami, R. Muto, M. Naruki, F. Sakuma, H. D. Sato, T. Tabaru,
S. Yamada, S. Yokkaichi** and Y. Yoshimura^{††}

Department of Physics, Kyoto University, Kitashirakawa Sakyo-Ku, Kyoto 606-8502, Japan

J. Chiba, M. Ieiri, M. Nomachi^{‡‡} , O. Sasaki, M. Sekimoto and K.H. Tanaka

Institute of Particle and Nuclear Studies, KEK, 1-1 Oho, Tsukuba, Ibaraki 305-0801, Japan

H. Hamagaki

*Center for Nuclear Study, Graduate School of Science, University of Tokyo, 7-3-1 Hongo, Tokyo
113-0033, Japan*

(December 15, 2000)

*Present Address: Center for Nuclear Study, Graduate School of Science, University of Tokyo,
7-3-1 Hongo, Tokyo 113-0033, Japan, email: ozawa@cns.s.u-tokyo.ac.jp

[†]Present Address: ICEPP, University of Tokyo, 7-3-1 Hongo, Tokyo 113-0033, Japan

[‡]Present Address: Physics Department, Graduate School of Science, Tohoku University, Sendai
980-8578, Japan

[§]Present Address: Fujitsu Corporation, 4-1-1, Kamikodanaka, Nakahara, Kawasaki, Kanagawa
211-8588, Japan

**Present Address: RIKEN, 2-1 Hirosawa, Wako, Saitama 351-0198, Japan

^{††}Present Address: Xaxon Corporation, 1-3-19, Tanimachi, Chu-ou, Osaka, Japan

^{‡‡}Present Address: Department of Physics, Osaka University, 1-1 Machikaneyama, Toyonaka,
Osaka 560-0043 , Japan

Abstract

We have measured the invariant mass spectra of electron-positron pairs in the target rapidity region of 12GeV p+A reactions. We have also observed a significant difference in the mass spectra below the ω meson between p+C and p+Cu interactions. The difference is interpreted as a signature of the ρ/ω modification at normal nuclear-matter density.

24.85.+p,25.30.-c

Recently, the chiral property of QCD in hot($T \neq 0$) or dense($\rho \neq 0$) matter has attracted wide interest in the field of hadron physics. The dynamical breaking of chiral symmetry in the QCD vacuum induces an effective mass of quarks, known as the constituent quark mass. In hot and/or dense matter this broken symmetry is subject to be restored either partially or completely and, hence, the properties of hadrons can be modified. To observe such an effect, measurements of the in-medium decay of vector mesons, especially in the lepton-pair channel, are highly desirable to directly obtain the meson properties in matter [1].

Although many heavy-ion experiments have been carried out in CERN-SPS and BNL-AGS to study hot and dense matter, there was only one experiment which could address the mass modification of vector mesons. The CERES/NA45 collaboration measured low-mass electron pair productions in Pb-Au collisions at 158 A GeV [2], and observed an enhancement of the e^+e^- pair yield in the mass range $0.3 < m_{ee} < 0.7$ GeV/ c^2 over the expected yield from the known hadronic sources in pp collisions. This striking effect could be understood as a consequence of the mass modification of a ρ and ω meson in hot matter.

In QCD, the mass of vector mesons, mainly determined by the effective mass of quarks, is closely related to $\bar{q}q$ condensates ($\langle\bar{q}q\rangle$), which is an order parameter of the chiral symmetry of the QCD vacuum. In this framework, a significant decrease of $\langle\bar{q}q\rangle$ is expected not only at high temperature, but also at normal nuclear density [3]. Using the QCD sum rule, Hatsuda and Lee theoretically predicted an in-medium modification of the vector mesons [4]. According to this model, the mass decrease at the normal nuclear density is $120 \sim 180$ MeV/ c^2 for the ω and ρ mesons and $20 \sim 40$ MeV/ c^2 for the ϕ meson. Thus, the measurements of such mesons, which are produced and decayed in a nucleus, are of great interest. The present experiment is one of several experimental efforts [1] to investigate the in-medium properties of the vector mesons at normal nuclear-matter density.

The present experiment, KEK-PS E325, was designed to measure the decays of the vector mesons, $\phi \rightarrow e^+e^-$, $\rho/\omega \rightarrow e^+e^-$ and $\phi \rightarrow K^+K^-$, in the kinematical region where the decay probability inside a target nucleus was enhanced ($0.6 < y_{ee} < 2.2$, $0.0 < P_{t ee} < 1.5$). The spectrometer was built at the primary beam line EP1B in the 12GeV-PS at KEK.

We have been taking data since 1998. This manuscript describes the e^+e^- triggered data of 5.6×10^7 events collected in 1998 using 2.2×10^{14} protons on the targets. The layout of the detectors is shown in Figure 1. The spectrometer had two electron arms and two kaon arms, which shared the dipole magnet and the tracking devices. The electron arms covered from $\pm 12^\circ$ to $\pm 90^\circ$ horizontally and $\pm 22^\circ$ vertically. The kaon arms covered from $\pm 12^\circ$ to $\pm 54^\circ$ horizontally and $\pm 6^\circ$ vertically. Primary protons with a typical intensity of 7×10^8 Hz were delivered to the targets at the center of the dipole magnet. We used three kinds of targets aligned in-line (carbon, polyethylene and copper) with interaction lengths of 0.028%, 0.061% and 0.020%, respectively. The carbon and copper targets were glued onto target supports made of paper ($C_6H_{12}O_6$), whose interaction length was 0.033%. The combination of an intense beam with a thin targets was essential to keep the gamma conversion rate below the Dalitz decay rate. The typical interaction rate was as high as 1.2 MHz.

Tracking was performed with a cylindrical drift chamber (CDC) and a barrel-shaped drift chambers (BDC). A dipole magnet having circular pole pieces of 880 mm in radius provided a field of 0.81 Tm from the center to 1600 mm in radius, where the BDC's were located. The acceptance of the CDC was from $\pm 12^\circ$ to $\pm 132^\circ$ horizontally and $\pm 22^\circ$ vertically, while the BDC had the same vertical coverage as the CDC with a smaller horizontal coverage of from $\pm 7.5^\circ$ to $\pm 94.5^\circ$. The CDC consisted of 10 layers of drift cells with an XX'U-VV'XX'-UXX' configuration covering the radial region from $r=445$ mm to $r=830$ mm. The BDC's had 4 layers with an XX'UV configuration, located at $r=1600$ – 1650 mm. In the X and the X' layers, the direction of the wires was vertical and in the U and V layers the wires were tilted by about ± 0.1 radian. All of the drift cells of the CDC had the same horizontal angular coverage of 1.5° with respect to the target, and the drift cells of the BDC had an angular coverage of 0.75° . Both the CDC and BDC used Argon-ethane mixed gas of 50% and 50% at 1 atm. The total thickness of the materials from the target to the front of BDC was 3.1% of the radiation length. A position resolution of $350 \mu m$ was obtained in the present analysis.

For electron identification the whole region of the electron arm was covered by two stages

of electron identification counters. The first stage of the electron identification was done by the front gas-Čerenkov counters (FGC), which covered from $\pm 12^\circ$ to $\pm 90^\circ$ horizontally and $\pm 23^\circ$ vertically. They were horizontally segmented into 13 units in each arm so that one segment covered 6° . The second stage consisted of three types of electron-identification counters, the rear gas-Čerenkov counters (RGC) which covered $\pm 12^\circ$ to $\pm 54^\circ$ horizontally and $\pm 6^\circ$ vertically with 7 horizontal segments in each arm. These regions corresponded to the kaon-arm acceptance. The rear lead-glass EM calorimeters (RLG) covered the same horizontal angle as the RGCs with 12 segments in each arm, but were vertically covered outside the kaon-arm acceptance, from $\pm 5^\circ$ to $\pm 23^\circ$. In the backward region, where the horizontal angle was larger than 57° , the second-stage electron identification was performed by side lead-glass EM calorimeters (SLG) which covered $\pm 57^\circ$ to $\pm 90^\circ$ horizontally and $\pm 23^\circ$ vertically with 9 horizontal segments in each arm.

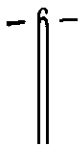
Both of the gas Čerenkov counters used iso-butane with a refractive index of 1.0019. The threshold momentum for pions was 2.3 GeV/c. Both the RLG and the SLG consisted of SF6W lead-glass. The typical energy resolution of the RLG and the SLG was $15\%/\sqrt{E}$. To suppress any fake triggers caused by pions and protons, we set the discriminator threshold for the gas Čerenkov counters higher than the optimum setting for electrons; thus, the electron efficiency was sacrificed. For electrons with a momentum greater than 400 MeV/c, the overall efficiencies, including the trigger threshold and the off-line cut, were 55% for FGC, 86% for RGC and 85% for the calorimeters, RLG and SLG. We achieved a pion rejection of 6.7×10^{-4} with a cascade operation of FGC and the EM calorimeters, and 3.9×10^{-4} with FGC and RGC for 400 MeV/c pions.

An electron trigger having three levels was adopted for the data accumulation. In the first level, we selected electron-pair candidates using the coincidence signal of the front-stage (FGC) and the rear-stage detectors (SLG, RLG, RGC), by requiring horizontal position matching. To suppress electron pairs with a small opening angle, such as from Dalitz decays and γ conversions, we required the two FGC hits to be more than 2 segmentations apart. In the second level, we required the pair to be oppositely charged by using the drift-chamber

hits associated with the FGC hits. The hit positions in the chambers were obtained from the OR-ed signal of the X and X' layers in the outer-most layers in CDC and in BDC. The OR-ed signals provided an effective angular segmentation of 1.5° both at $r=825$ mm (CDC) and $r=1605$ mm (BDC). The sign of a track can be roughly determined with these segmentations together with the target position. We eliminated the electron-pair candidates which had an apparent “++” or “--” configuration. We also required the remaining pairs to be more than 12° apart at the $r=825$ mm position to suppress electron pairs with a small opening angle. In the third level, the approximate opening angles of the pairs were calculated. Because the radius of the BDC layers was almost two times larger than the radius of the outer-most CDC layers, the opening angle of the pair at the target, Θ_{open} , could be approximated by $\Theta_{open} = 2 \times \Theta_{cdc} - \Theta_{bdc}$, where Θ_{cdc} is the opening angle of the pair at the outer-most CDC layer and Θ_{bdc} at the BDC layer with respect to the target position. We required Θ_{open} to be in the range from 50° to 150° in the trigger. The typical trigger rates were 450, 330 and 280 Hz in the first, second and third level triggers, respectively. We kept the live time of the data acquisition at around 60%.

To evaluate the performance of the spectrometer, the mass resolution was examined for the observed peaks of the $\Lambda \rightarrow p + \pi^-$ and $K_s \rightarrow \pi^+ + \pi^-$ decays, as shown in Figures 2a and 2b. For the Λ peak we obtained the centroid at $1115.5 \text{ MeV}/c^2$ (known to be $1115.7 \text{ MeV}/c^2$) with a Gaussian resolution of $1.8 \pm 0.1 \text{ MeV}/c^2$, and for K_s , $493.9 \text{ MeV}/c^2$ (known to be $497.7 \text{ MeV}/c^2$) and $3.6 \pm 0.6 \text{ MeV}/c^2$, respectively. The observed peak positions and widths give the systematic uncertainty of the mass scale and the mass resolution of the present analysis. The results were compared to Monte-Carlo simulations in which we took the chamber resolution and the multiple scattering into account. The observed widths were well reproduced by the simulation ($1.9 \text{ MeV}/c^2$ for Λ and $3.5 \text{ MeV}/c^2$ for K_s), and the energy scale uncertainty for the ω and ϕ meson was estimated to be $4 \text{ MeV}/c^2$ and $7 \text{ MeV}/c^2$ and the mass resolution to be $9.6 \text{ MeV}/c^2$ and $12.0 \text{ MeV}/c^2$, respectively.

Figure 3 shows the e^+e^- invariant mass spectra: (a) for the carbon and polyethylene targets (light nuclear targets) and (b) for the copper target (heavy nuclear target). These



histograms contain the events when the electron and the positron are detected in different arms, so that the low-mass part of the spectra is largely suppressed. Although the clear peaks of the ω meson decaying into e^+e^- are visible in the spectra, a significant shape difference is observed between the light nuclear targets and the copper target, and an excess at the low mass side of the ω peak can be seen.

We tried to reproduce the mass shape of the obtained histograms with the combinatorial background and the known hadronic sources. The origins of the combinatorial background were pairs which were picked up from two independent Dalitz decays or γ conversions, and pairs like $e^-\pi^+$ or $e^+\pi^-$ due to mis-identification. The remaining $e^-\pi^+$ and $e^+\pi^-$ background was estimated to be about 13% in the spectra and the contaminations like $\pi^+\pi^-$ to be negligibly small. The distribution of the combinatorial background was obtained from the event-mixing method. As known hadronic sources, $\rho \rightarrow e^+e^-$, $\omega \rightarrow e^+e^-$, $\phi \rightarrow e^+e^-$, $\eta \rightarrow e^+e^-\gamma$ and $\omega \rightarrow e^+e^-\pi^0$ were considered. The Dalitz decay, $\pi^0 \rightarrow e^+e^-\gamma$, is negligible in the mass acceptance of the present data. The shapes of the e^+e^- invariant mass spectra from the Dalitz decays, $\eta \rightarrow e^+e^-\gamma$ and $\omega \rightarrow e^+e^-\pi^0$, were taken from reference [5]. The mass shape of the ρ , ω and ϕ mesons was given as the Breit-Weigner function with the natural width 150 MeV/c², 8.41 MeV/c² and 4.43 MeV/c², respectively. The Breit-Weigner functions were smeared with the estimated mass resolution of 9.6 MeV/c² for the ω and 12.0 MeV/c² for the ϕ meson. Because the present experiment used targets with a radiation length of less than 0.3%, the radiative tail and the multiple scattering due to the target thickness were negligible. We assumed that the production cross section of ρ is equal to that of ω [6]. To obtain the mass shape of the known sources in the observed spectra, we evaluated the experimental mass acceptance using the particle distributions obtained by the nuclear cascade code, JAM [7].

The relative abundances of the known sources and the combinatorial background were obtained through fitting with four parameters, the amplitudes of $\rho/\omega \rightarrow e^+e^-$, $\phi \rightarrow e^+e^-$, $\eta \rightarrow \gamma e^+e^-$ and the combinatorial background. The amplitude of the other source, $\omega \rightarrow \pi^0 e^+e^-$, was given by the branching ratio. The best fits are over-plotted in Figure 3. The

contribution of $\eta \rightarrow \gamma e^+ e^-$ turned out to be negligible. As a result of the fits, we found 75.5 ± 9.0 ω mesons and 7.4 ± 5.8 ϕ mesons from the light target and 20.0 ± 4.8 ω mesons and 5.2 ± 2.7 ϕ mesons from the copper target. The invariant mass shapes were well reproduced, except for the mass region below the omega peak.

To evaluate the excess in the mass region from $550 \text{ MeV}/c^2$ to $750 \text{ MeV}/c^2$, we fit the histograms again while excluding this mass region. The excess was estimated by subtracting the amplitude of the fit function from the data. The number excess of the light target was 19.6 ± 11.7 and that of the copper target was 29.5 ± 8.7 . The excess is statistically significant for the copper target data. The ratios to the amplitude of the omega peak are 0.26 ± 0.16 for the light target and 1.48 ± 0.56 for the copper target. The difference between the two cases should have originated from the difference in the nuclear size. A natural explanation for the shape change is that the mass modification of ρ/ω mesons takes place inside a nucleus. Although the mass shape of the modified meson is difficult to predict, it should be noted that the excess in the copper target data is visible in the mass range about 200 MeV below the ω peak. This range is consistent with the expected shift predicted by Hatsuda and Lee [4].

In summary, we have observed a signature of in-medium mass modification of ρ/ω meson. This is the first observation of the leptonic in-medium decay of vector mesons at normal nuclear-matter density.

Acknowledgements We would like to thank all of the staff members of KEK PS, especially for the helpful support by the beam channel group. This work was partly supported by the Japan Society for the Promotion of Science and a Grant-in-Aid for Scientific Research of the Japan Ministry of Education, Science and Culture (Monbusho).

REFERENCES

- [1] W. Schoen *et al.* (HADES Collaboration), Acta Phys. Polon. **B27**:2959-2963 (1996).
G.J. Lolos *et al.* (TAGX Collaboration), Phys. Rev. Lett. **80**:241-244 (1998).
GSI/SIS proposal S214, Search for bound η - and ω - nuclear states using the recoilless ($d, {}^3\text{He}$) reaction.
T. Nakano *et al.*, Nucl. Phys. **A629**, 559c (1998).
KEK-PS E325 proposal
(http://www.pn.scphys.kyoto-u.ac.jp/phi/E325_project.html).
- [2] G. Agakichiev *et al.*, Phys. Lett. **B422** (1998) 405.
- [3] E.G. Drukarev and E.M. Levin, Prog. Part. Nucl. Phys. **27** (1991) 77.
- [4] T. Hatsuda and S. H. Lee, Phys. Rev. **C46** (1992) R24.
- [5] A. Faessler, C. Fuchs and M. I. Krivoruchenko, Phys. Rev. **C61**:035206 (2000).
- [6] V. Blobel *et al.*, Phys. Lett. **B48**, 73 (1974).
- [7] Y. Nara *et al.*, Phys. Rev. **C61**:024901 (1999).

FIGURES

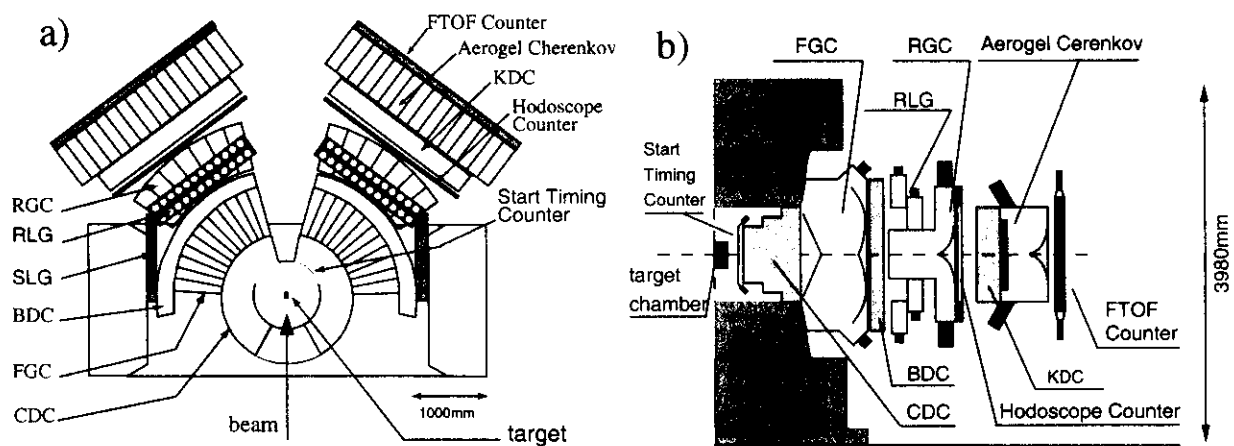


FIG. 1. Schematic view of the experimental setup of the E325 spectrometer: (a) for the top view and (b) for the side view. The side view shows the cross section along the center of the kaon arm (see text).

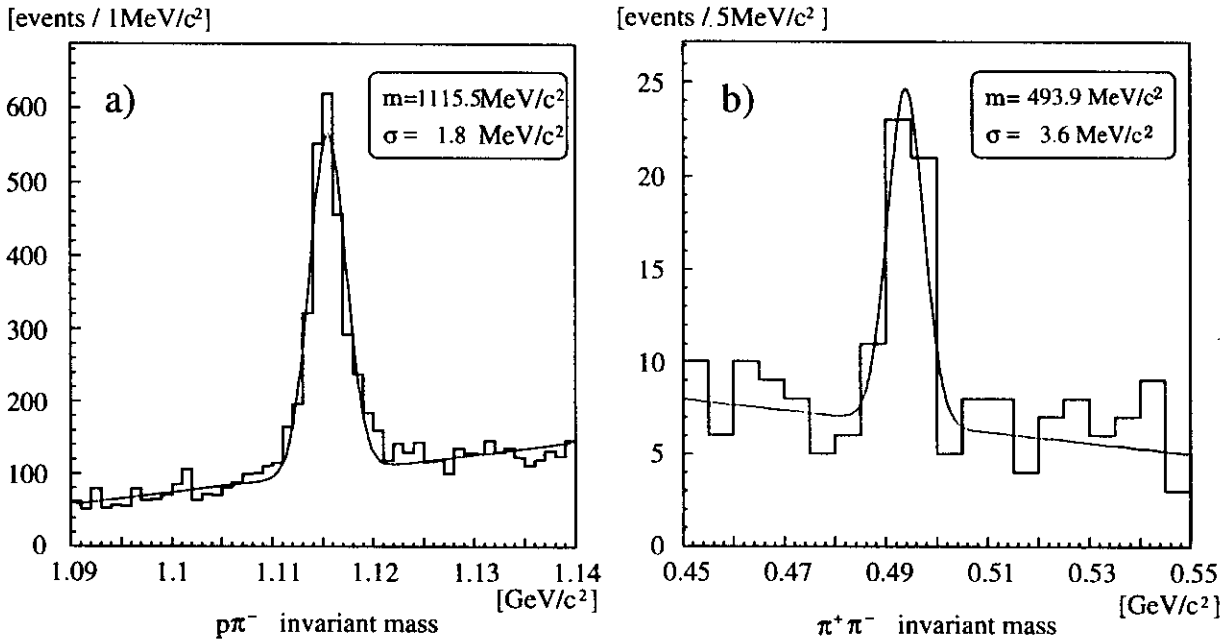


FIG. 2. Invariant mass spectrum of $p\pi^-$ (a) and $\pi^+\pi^-$ (b). The lines are the best-fit results by applying a Gaussian with a linear background. The vertex position of $p\pi^-$ pairs were required to be more than 20 mm apart from the target and of $\pi^+\pi^-$ pairs more than 10mm.

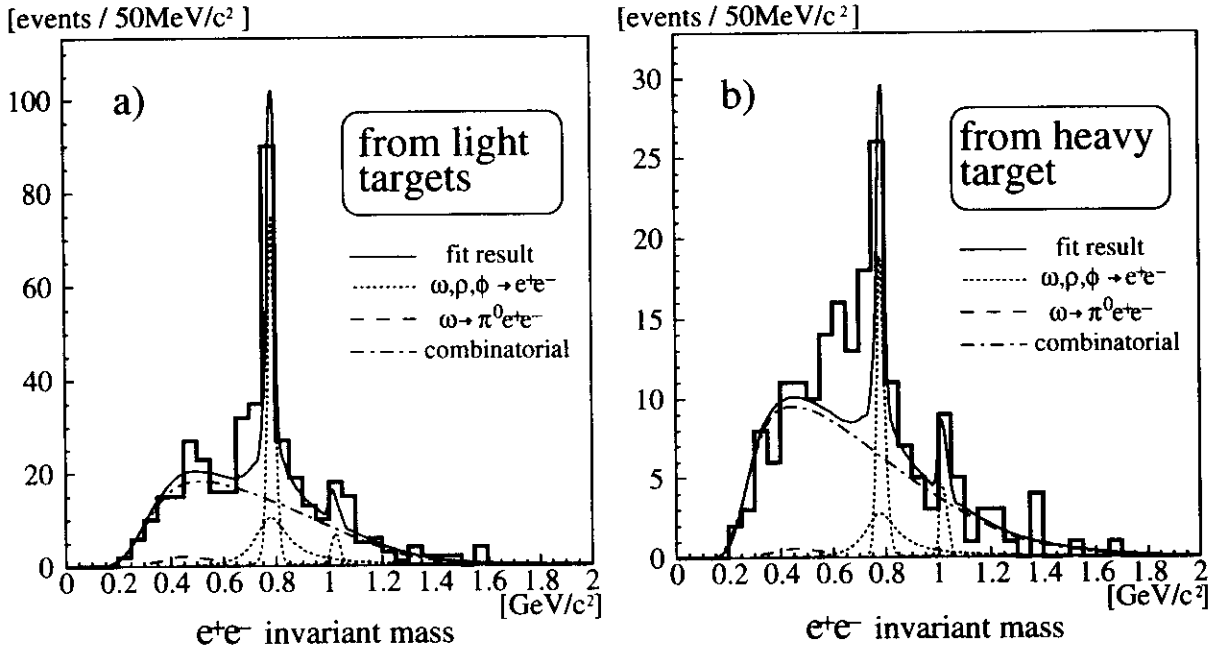


FIG. 3. Invariant mass spectrum of e^+e^- pair: (a) for the carbon and polyethylene targets and (b) for the copper target. The solid lines show the best-fit results of the known hadronic sources with the combinatorial background. The dotted lines are the contribution from ρ , ω and ϕ decays. The dashed lines are for $\omega \rightarrow \pi^0 e^+e^-$ decays and the dot-dashed lines are for the combinatorial background.